Synthesis of Oxadiazole-Based Polymers Containing a Carbazole–Vinylene or Fluorene–Vinylene Group and Their Hole-Injection/Transport Behavior in Light-Emitting Diodes

Hui Wang,[1] Jeong-Tak Ryu,[1] Younghwan Kwon[2]

[1]*College of Information and Communication Engineering, Daegu University, Gyeongsan, Gyeongbuk 712-714, Korea*
[2]*Department of Chemical Engineering, Daegu University, Gyeongsan, Gyeongbuk 712-714, Korea*

Received 31 December 2009; accepted 12 April 2010
DOI 10.1002/app.32647
Published online 27 July 2010 in Wiley Online Library (wileyonlinelibrary.com).

ABSTRACT: A series of conjugated (poly{*N*-(2-ethylhexyl)-3,6-carbazole–vinylene-*alt*-[(2,5-bisphenyl)-1,3,4-oxadiazole]}) and nonconjugated (poly{*N*-(2-ethylhexyl)-3,6-carbazole–vinylene-alt-[(2,5-bisphenol)-1,3,4-oxadiazole]}) and poly{9,9-dihexyl-2,7-fluorene–vinylene-*alt*-[(2,5-bisphenol)-1,3,4-oxadiazole]}) polymers containing oxadiazole and carbazole or fluorene moieties in the polymer backbone were synthesized with a multiple-step procedure. The properties of the polymers, including the photophysical and electrochemical characteristics, could be fine-tuned by adjustment of the components or structures in the polymer chains. The polymers were used to examine the hole-injection/transport behavior as hole-injection/hole-transport layers in double-layer indium tin oxide (ITO)/polymer/aluminum tris(8-hydroxyquinoline)/LiF/Al devices by the determination of their energy levels. The effects of the polymers in these devices on the charge-transport behavior were compared with a control device fabricated with poly(ethylenedioxythiophene) (PEDOT)–poly(styrene sulfonate) (PSS). Devices containing the synthesized polymers showed comparable adhesion to the ITO anode and good hole-injection/transport performance. In addition, they exhibited higher electroluminescence over an identical range of current densities than the control device. This was attributed to the prevention of radiative exciton quenching caused by the PEDOT–PSS interfaces and the improvement of electron/exciton blocking due to the higher electron affinity of the synthesized polymers. © 2010 Wiley Periodicals, Inc. J Appl Polym Sci 119: 377–386, 2011

Key words: charge transport; conjugated polymers; light-emitting diodes (LED); luminescence

INTRODUCTION

Polymer light-emitting diodes (PLEDs) have attracted considerable attention as flat-panel displays because of their advantages, such as the possibility of fabrication over a large area on a flexible substrate and their very low cost.[1,2] Generally, PLEDs consist of several layers, depending on their functions, such as a hole-injection layer (HIL) and/or hole-transport layer (HTL), emitting layer (EML), and electron-injection layer and/or electron-transport layer, which are sandwiched between two electrodes. Polymers are considered to be highly disordered states having prevailing charge traps with intrinsic origins (e.g., structural defects) and extrinsic origins (e.g., chemical impurities); these result in poor charge-injection/transport properties. Therefore, efficient, balanced charge injection and transport behaviors between the layers are some of the key parameters in the achievement of practical applications of PLEDs. From the standpoint of materials, efforts have been made to produce devices with balanced charge-injection/transport characteristics with a range of polymers by the design of molecular moieties, including fluorene, carbazole, phenylene, oxadiazole, and its derivatives,[3–6] and through the use of a variety of polymerization techniques, such as Suzuki coupling[7] and Yamamoto,[3] Heck,[8] and Wittig reactions.[9] Another approach from the device point of view has been the judicious matching of energy barrier levels and appropriate interfacial contacts in each layer of the devices. This is because the interfaces between the electrode and polymer and polymer and polymer are crucial for charge injection/transport and the determination of their operating characteristics and stability. Although much study of these interfaces has been done,[10,11] they are still poorly understood.

Poly(ethylene dioxythiophene) (PEDOT)–poly(styrene sulfonate) (PSS) has a reasonable ionization potential ($I_p = -5.2$ to -5.3 eV), high conductivity ($\sim$ 1–10 S/cm), and good stability.[12–14] It has been incorporated to accommodate a large hole-injection barrier (ϕ_h) between the indium tin oxide (ITO) anode (-4.5

Correspondence to: Y. Kwon (y_kwon@daegu.ac.kr).
Contract grant sponsor: Daegu University Research Grant 2010.

eV of Fermi level as received), an organic HTL or EML [far below −5.0 eV of I_p], and a surface-energy mismatch (hydrophilic ITO vs most hydrophobic organic HTLs and EMLs). However, limited hole-injection behavior at the interface of PEDOT–PSS/light-emitting polymers in PLEDs has been often reported[15,16] to be attributed mainly to nonohmic contact as a result of a surface-energy mismatch between two layers rather than by the hole-injection energy barrier. Another important but detrimental process occurring at this interface was found to be radiative exciton quenching by the PEDOT–PSS layer; this led to a significant decrease in the interfacial luminescence quantum yield of the devices.[14,17–20] These interfacial issues could be prevented by the incorporation of a nanoscale interfacial layer between the PEDOT–PSS and light-emitting polymer layers.[18,21] However, Harding et al.[22] reported that the addition of an interlayer between the PEDOT–PSS and light-emitting polymers improved the device performance but also required additional, complex considerations, such as physical contact, intermixing, and trapping, at the PEDOT–PSS/interlayer/light-emitting polymer boundary. The device performance appears to be improved with the increasing complexity of the devices by the incorporation of more interlayers with respective functions (e.g., for the ohmic contact at the interfaces, for aligned energy levels at each layer, for preventing the radiative quenching of excitons at the interfaces), as mentioned previously. However, there is no doubt that a simple device structure is preferred. The simplicity of the device structure, one of the most important features of PLEDs, has been endeavored by the integration of distinct functions, such as charge injection/transport and light emitting, into the chemical structure of the materials in PLEDs. For instances, electroluminescent conjugated copolymers containing electron-transporting oxadiazole groups and hole-transporting carbazole or fluorine units have been reported.[23,24]

In this study, a series of carbazole–vinylene and fluorene–vinylene containing oxadiazole-based polymers were designed to evaluate the performance of polymers as HILs/HTLs and for good interfacial contact with ITO in devices. A conjugated copolymer [poly{*N*-(2-ethylhexyl)-3,6-carbazole–vinylene-*alt*-[(2,5-bisphenyl)-1,3,4-oxadiazole]} (**P1**)] containing *N*-(2-ethylhexyl)-3,6-carbazole–vinylene and 1,3,4-oxadiazole groups was synthesized by a Wittig reaction. Two nonconjugated copolymers [poly{*N*-(2-ethylhexyl)-3,6-carbazole–vinylene-*alt*-[(2,5-bisphenol)-1,3,4-oxadiazole]} (**P2**) and poly{9,9-dihexyl-2,7-fluorene–vinylene-*alt*-[(2,5-bisphenol)-1,3,4-oxadiazole]} (**P3**)], with a flexible aryl ether unit consisting of *N*-(2-ethylhexyl)-3,6-carbazole–vinylene for **P2** or 9,9-dihexyl-2,7-fluorene–vinylene for **P3,** and 1,3,4-oxadiazole groups were prepared by nucleophilic polycondensation. The photophysical and electrochemical characteristics of these polymers are presented in detail. In addition, the effects of the synthesized polymers as HILs/HTLs on the device performance were evaluated comparatively with commercialized PEDOT–PSS.

EXPERIMENTAL

Materials

Phosphorus oxychloride ($POCl_3$), poly(phosphoric acid) (PPA), 4-acetoxystyrene, palladium(II) acetate, triphenylphosphine (PPh_3), 4-fluorobenzoic acid, and hydrazine sulfate were purchased from Aldrich Co. (St. Louis, MO) and were used as received. *N*-(2-Esthylhexyl)carbazole (**1**) was synthesized from a carbazole with a procedure reported in the literature.[25] 2,5-Bis[(*p*-bromomethyl)phenyl]-1,3,4-oxadiazole (**4**) was prepared from *p*-toluoylchloride and *p*-toluichydrazide.[26] 3,6-Dibromo-*N*-(2-ethylhexyl)carbazole (**6**) and 2,7-dibromo-9,9-di-*n*-hexylfluorene (**8**) were prepared with a procedure reported elsewhere.[27,28] The other reagents were supplied by TCI Chemical Co. and were used without further purification. The solvents were purified with normal procedures and handled under moisture-free conditions.

3,6-Diformyl-*N*-(2-ethylhexyl)carbazole (monomer 1)

$POCl_3$ (25.5 mL) was added dropwise to a flask containing dimethylformamide (DMF; 22 mL) over a period of 0.5 h at 0°C under a nitrogen atmosphere. The deep red solution obtained was warmed to room temperature and stirred for 3 h. A solution of compound **1** (4.19 g, 15.1 mmol) in 1,2-dichloroethane (18 mL) was added dropwise to the mixture. The mixture was heated to 90°C and stirred for 48 h. The dark reaction products were poured into water, stirred overnight at room temperature, neutralized with sodium bicarbonate, and extracted with dichloromethane. The organic layer was washed with water, dried over $MgSO_4$, and concentrated. The crude product was purified by column chromatography on silica with a solvent mixture (dichloromethane/ethyl acetate = 99/1 v/v). A yellow solid was obtained at 50% yield.

^{1}H-NMR (300 MHz in $CDCl_3$, δ): 10.14 (s, 2H, CHO), 8.67 (s, 2H, Ar—H), 8.10–8.07 (d, 2H, Ar—H), 7.55–7.52 (d, 2H, Ar—H), 4.25 (m, 4H, —N—CH_2—), 2.05 (s, 1H,—CH—), 1.44–1.21 (m, 8H, —CH_2—), 0.91 (m, 6H, —CH_3). ^{13}C-NMR (300 MHz in $CDCl_3$, δ): 191.6, 145.2, 129.6, 127.9, 124.3, 123.1, 110.1, 60.4, 48.0, 39.4, 30.9, 28.7, 24.3, 23.0, 14.0, and 10.9. Gas chromatography (GC)–mass spectroscopy (MS): m/z = 335 (m+).

2,5-Bis{[(*p*-triphenylphosphonio)methyl]phenyl}-1,3-4-oxadiazole (monomer 2)

Compound **4** (2 g, 7.2 mmol) and PPh_3 (3 g, 11.2 mmol) were added to a two-necked flask containing DMF (33 mL), heated to 110°C, and stirred overnight under nitrogen. The precipitate was filtered and washed with diethyl ether (45 mL) to obtain the phosphonium salts at an 80% yield.

^{1}H-NMR (300 MHz in $CDCl_3$, δ): 7.9–7.45 (m, 30H, Ar—H), 7.35 (d, 4H, Ar—H), 7.2 (d, 4H, Ar—H), 6.15 (s, 2H, —CH_2—), 6.11 (s, 2H, —CH_2—). ^{13}C-NMR (300 MHz in $CDCl_3$, δ):163.9, 135.6, 134.5, 134.4, 132.8, 132.7, 132.2, 130.6, 130.5, 127.3, 123.3, 118.5, 117.3. GC–MS: $m/z = 930$ (m+)

N-(2-Ethylhexyl)-3,6-bis(4-acetoxylstyryl)carbazole (9) and 9,9-dihexyl-2,7-bis(4-acetoxylstyryl) fluorene (10)

The Heck reaction was carried out for the synthesis of compounds **9** and **10**. Compound **6** (1.44 g, 3.3 mmol) was used for the synthesis of compound **9** [and compound **8** (1.62 g) was used for the synthesis of compound **10**]. Compound **6,** 4-acetoxystyrene (1.42 g, 8.2 mmol), palladium(II) acetate (0.15 g, 0.2 mmol), PPh_3 (0.38 g, 1.2 mmol), triethylamine (3.3 mL), and DMF (8 mL) were added to a two-necked flask and stirred at 90°C for 48 h under a nitrogen atmosphere. After cooling, the reaction mixture was poured into distilled water and neutralized by the addition of an aqueous HCl solution. The mixture was extracted with chloroform, washed with distilled water, dried with anhydrous $MgSO_4$, and then concentrated. The residue was purified by chromatography on a silica gel with a mixture eluent (hexane/ethyl acetate = 9/1 v/v) to give a yellow product (yield = 40%). The procedure used for compound **10** was similar to that used for compound **9,** and a yellow compound was produced at a 38% yield.

Compound **9:** ^{1}H-NMR [300 MHz in hexadeuterated dimethylsulfoxide (DMSO-d_6)]: 8.40 (s, 2H, Ar—H), 7.70 (d, 2H, Ar—H), 7.66 and 7.64 (d, 4H, Ar—H), 7.57 and 7.55 (d, 2H, Ar—H), 7.42 (d, 4H, vinyl H), 7.15 and 7.13 (d, 4H, Ar—H), 4.28 (d, 2H, —NCH_2—), 2.28 (s, 6H,—CH_3), 1.97 (s, 1H, —CH—), 1.40 (m, 8H, —CH_2—), 0.87–0.75 (m, 6H, —CH_3). GC–MS: $m/z = 599$ (m+).

Compound **10:** ^{1}H-NMR (300 MHz in DMSO-d_6, δ): 7.80 (d, 2H, Ar—H), 7.68 (m, 6H, Ar—H), 7.58 (d, 2H, Ar—H), 7.32 (d, 4H, vinyl H), 7.15 (d, 4H, Ar—H), 2.27 (s, 6H, —CH_2—), 2.0 (m, 4H, —CH_2—), 1.06–0.98 (m, 12H, —CH_2—), 0.7 (t, 6H, —CH_3), 0.53 (s, 4H, —CH_2—). GC–MS: $m/z = 654$ (m+).

N-(2-Ethylhexyl)-3,6-bis(4-phenol)carbazole (monomer 3) and [9,9-dihexyl-2,7-bis(4-phenol)] fluorene (monomer 4)

Bisphenol monomer **3** (or monomer **4**) was obtained by the hydrolysis and acidification of compound **9** (or compound **10**). A mixture of compound **9** (1.2 g, 2 mmol) and KOH (1 g, 10% in water) was dissolved in 20 mL of ethyl alcohol. The reaction mixture was then heated to 80°C and stirred for 5 h in a nitrogen atmosphere. The resulting mixture was poured into distilled water and then acidified by the addition of an aqueous HCl solution. The residue was purified by column chromatography on a silica gel with 9/1 v/v hexane/ethyl acetate as the eluent to afford pale powder of monomer **3** at a 75% yield. The procedure used for monomer **4** was similar to that of monomer **3,** and a yellow powder was obtained at a 90% yield.

Monomer **3:** ^{1}H-NMR (300 MHz in DMSO-d_6, δ): 9.56 (s, 2H, —OH), 8.36 (s, 2H, Ar—H), 7.68–7.65 (d, 2H, Ar—H), 7.53–7.5 (d, 2H, Ar—H), 7.46–7.43 (d, 4H, Ar—H), 7.18 (s, 4H, vinyl H), 6.81–6.78 (d, 4H, Ar—H), 4.25 (d, 2H, —NCH_2—), 1.97 (m, 1H, —CH—), 1.31–1.16 (m, 8H, —CH_2—), 0.88–0.76 (m, 6H, —CH_3). ^{13}C-NMR (DMSO-d_6, δ): 156.9, 140.2, 128.8, 128.7, 127.5, 126.1, 125.8, 124.6, 122.5, 117.9, 115.6, 109.8, 30.7, 28.0, 22.5, 13.9, 10.7. GC–MS: $m/z = 515$ (m+).

Monomer **4:** ^{1}H-NMR (300 MHz in DMSO-d_6, δ): 9.60 (s, 2H, —OH), 7.74–7.72 (d, 2H, Ar—H), 7.60 (s, 2H, Ar—H), 7.55–7.39 (m, 6H, Ar—H), 7.19 (s, 2H, vinyl H), 7.11 (s, 2H, vinyl H), 6.79 (d, 4H, Ar—H), 2.03 (s, 4H, —CH_2—), 1.05–0.99 (m, 12H,—CH_2—), 0.72–0.68 (m, 6H,—CH_3), 0.52 (m, 4H, —CH_2—). ^{13}C-NMR (DMSO-d_6, δ): 157.3, 150.8, 142.5, 139.6, 136.6, 132.2, 131.1, 128.4, 127.8, 125.8, 125.3, 120.0, 115.6, 54.5, 31.0, 29.0, 23.5, 22.0, 13.9. GC–MS: $m/z = 570$ (m+).

2,5-Bis(*p*-fluorophenyl)-1,3,4-oxadiazole (monomer 5)

Bisfluoride monomer **5** was synthesized from 4-fluorobenzoic acid and hydrazine sulfate. 4-Fluorobenzoic acid (2.8 g, 20 mmol), hydrazine sulfate (1.3 g, 10 mmol), and PPA (25 mL) were added to a two-necked flask. The mixture was heated to 150°C for 4 h, then heated to 200°C, and reacted for a further 2 h. The solution was precipitated in water (200 mL), and the solids were filtered and dried (yield = 90%).

^{1}H-NMR (300 MHz in acetone-d_6, δ): 8.27–8.22 (d, 4H, Ar—H), 7.44–7.38 (d, 4H, Ar—H). ^{13}C-NMR (300 MHz in acetone-d_6, δ): 130.2, 130.1, 117.4, 117.1. GC–MS: $m/z = 258$ (m+).

P1

A solution of sodium (0.28 g, 12 mmol) in anhydrous ethanol (16 mL) was added under nitrogen to a mixture of monomer **1** (1.34 g, 4 mmol) and monomer **2** (3.73 g, 4 mmol) in anhydrous ethanol/chloroform (64 mL, 5/3 v/v). The mixture was stirred

overnight at room temperature. The polymerization was quenched by the addition of dilute HCl (2% in water) and stirred. The product was collected and washed with ethanol/water (9/1 v/v). The resulting product was dissolved in chloroform, precipitated in ethanol several times, and dried *in vacuo*.

^{1}H-NMR (300 MHz in $CDCl_3$, δ): 7.96–7.70 (m, 6H, Ar—H), 7.71–7.19 (m, 8H, Ar—H), 6.89 (d, 2H, vinyl H), 6.58 (d, 2H, vinyl H), 4.07 (s, 2H, —NCH_2—), 2.02 (s, 1H, —CH—), 1.5–1.1 (m, 8H, —CH_2—), 1.0–0.6 (m, 6H, —CH_3). ^{13}C-NMR (300 MHz in $CDCl_3$, δ): 164.28, 144.77, 141.42, 141.25, 140.95, 140.63, 134.5, 132.91, 132.12, 131.99, 131.57, 130.24, 129.4, 128.97, 128.6, 128.06, 127.57, 127.07, 126.77, 125.8, 124.62, 124, 123.04, 122.88, 122.74, 121.93, 120.91, 119.04, 109.35, 109.02, 74.12, 47.52, 39.35, 30.91, 28.66, 24.32, 22.99, 13.96, 10.8.

P2 and P3

Two polymers were prepared as follows. Bisfluoride monomer (0.50 mmol), bisphenol monomer (0.50 mmol), toluene (5 mL), *N*-methylpyrrolidone (NMP; 2.5 mL), and an excess of K_2CO_3 (1.20 mmol) were added to a two-necked flask. The reaction was kept at 160°C for 24 h. After the toluene was removed, the reaction mixture was dropped into a methanol/distilled water (250 mL, 2/1 v/v) mixture. The precipitates were collected by filtration and dried *in vacuo*.

P2: ^{1}H-NMR (300 MHz in $CDCl_3$, δ): 8.23 (s, 2H, Ar—H), 8.10 (s, 4H, Ar—H), 7.58 (d, 6H, Ar—H), 7.36–7.0 (m, 14H, Ar—H, vinyl H), 4.15 (s, 2H, —NCH_2—), 2.01 (s, 1H, —CH—), 1.5–1.12 (m, 8H, —CH_2—), 1.0–0.8 (m, 6H, —CH_3). ^{13}C-NMR (300 MHz in $CDCl_3$, δ): 163.95, 160.67, 154.59, 141.02, 134.46, 129.35, 128.73, 128.52, 127.69, 124.99, 124.55, 123.12, 120.21, 118.54, 119.2, 109.37, 66.41, 47.53, 39.40, 30.91, 28.75, 24.32, 23.02, 14.0, 10.9.

P3: ^{1}H-NMR (300 MHz in $CDCl_3$, δ): 8.13–8.10 (d, 4H, Ar—H), 7.69–7.67 (d, 4H, Ar—H), 7.61–7.59 (d, 4H, Ar—H), 7.53–7.48 (m, 4H, Ar—H), 7.23–7.1 (m, 12H, Ar—H, vinyl H), 2.01 (m, 4H, —CH_2—), 1.07 (m, 8H, —CH_2—), 0.78–0.69 (m, 6H, —CH_3). ^{13}C-NMR (300 MHz in $CDCl_3$, δ): 165.2, 161.72, 156.2, 152.7, 141.81, 137.3, 135.19, 130.35, 129.9, 129.1, 127.99, 126.79, 121.83, 121.3, 121.1, 119.66, 119.55, 56.13, 32.66, 30.89, 24.9, 23.75, 15.18.

Characterization of the materials

The ^{1}H-NMR and ^{13}C-NMR spectra were recorded with a Varian Unity Plus 300 spectrometer (Palo Alto, CA), and the chemical shifts were recorded in parts per million. The GC–MS spectra were collected on a QP 5050 mass spectrometer (Shimadzu Co., Tokyo, Japan). The molecular weights and molecular weight distributions of the polymers were measured by a gel permeation chromatograph (Waters Co., Milford, MA) equipped with a Styragel HR 5E column with tetrahydrofuran (THF) as the eluent against polystyrene standards. Thermogravimetric analysis (TGA) was performed under a nitrogen atmosphere at a heating rate of 10°C/min with a DuPont 9900 analyzer (Wilmington, DE). The ultraviolet–visible (UV–vis) spectra were recorded on a Shimadzu UV-2100 spectrophotometer (Tokyo, Japan), and the photoluminescence (PL) spectra were measured on a Shimadzu RF-5301PC fluorimeter, in both the solution and the solid state. Cyclic voltammetry was performed on a BAS100W electrochemical instrument (Bioanalytical Systems, Inc., West Lafayette, IN) with a three-electrode cell in a solution of Bu_4NBF_4 (0.10*M*) in acetonitrile at a scan rate of 50 mV/s. I_p was measured by photoelectron spectroscopy (Riken Keiki AC-2, Tokyo, Japan).

Fabrication of the Devices

OLEDs were fabricated with the following configuration: ITO/polymers/aluminum tris(8-hydroxyquinoline) (Alq_3; 60 nm)/LiF (1 nm)/Al (100 nm). First, a polymer film was spin-coated onto ITO glass from a polymer solution in 1,1,2,2-tetrachloroethane (1 wt %) to produce an approximately 30–40 nm thick HIL/HTL. Alq_3 was then deposited on the surface of the polymer film. Finally, LiF and Al were deposited by thermal evaporation. In these devices, the ITO-coated glass was cut to 5.0 × 5.0 cm^2, and the electrode area was prepared with a photoetching technique. The base vacuum for evaporation was less than 10^{-6} torr. The current density (*I*)–voltage (*V*)–luminescence (*L*) characteristics were measured with a direct-current power supply connected to a model 8092A digital multimeter and luminance meter (Minolta LS-100, Konica Minolta sensing, Inc., Tokyo, Japan).

RESULTS AND DISCUSSION

Synthesis and characterization

P1 was synthesized from a dialdehyde and a diphosphonium salt in a mixed ethanol/chloroform solvent with the Wittig reaction, as shown in Scheme 1. **P2** and **P3** with flexible ether groups in the polymer backbone were prepared from the nucleophilic polycondensation of a bisphenol and bisfluoride according to Scheme 2. The structural homogeneity of the polymers was identified by ^{1}H-NMR and ^{13}C-NMR. For example, we traced **P1** by monitoring the proton signals of the dialdehyde (monomer **1**) at 10.2 and 10.5 ppm in the ^{1}H-NMR spectrum. The disappearance of the peaks indicated the complete consumption of the monomer. For **P2** and **P3,** the disappearance of hydroxyl protons at 9.6 ppm was also monitored to

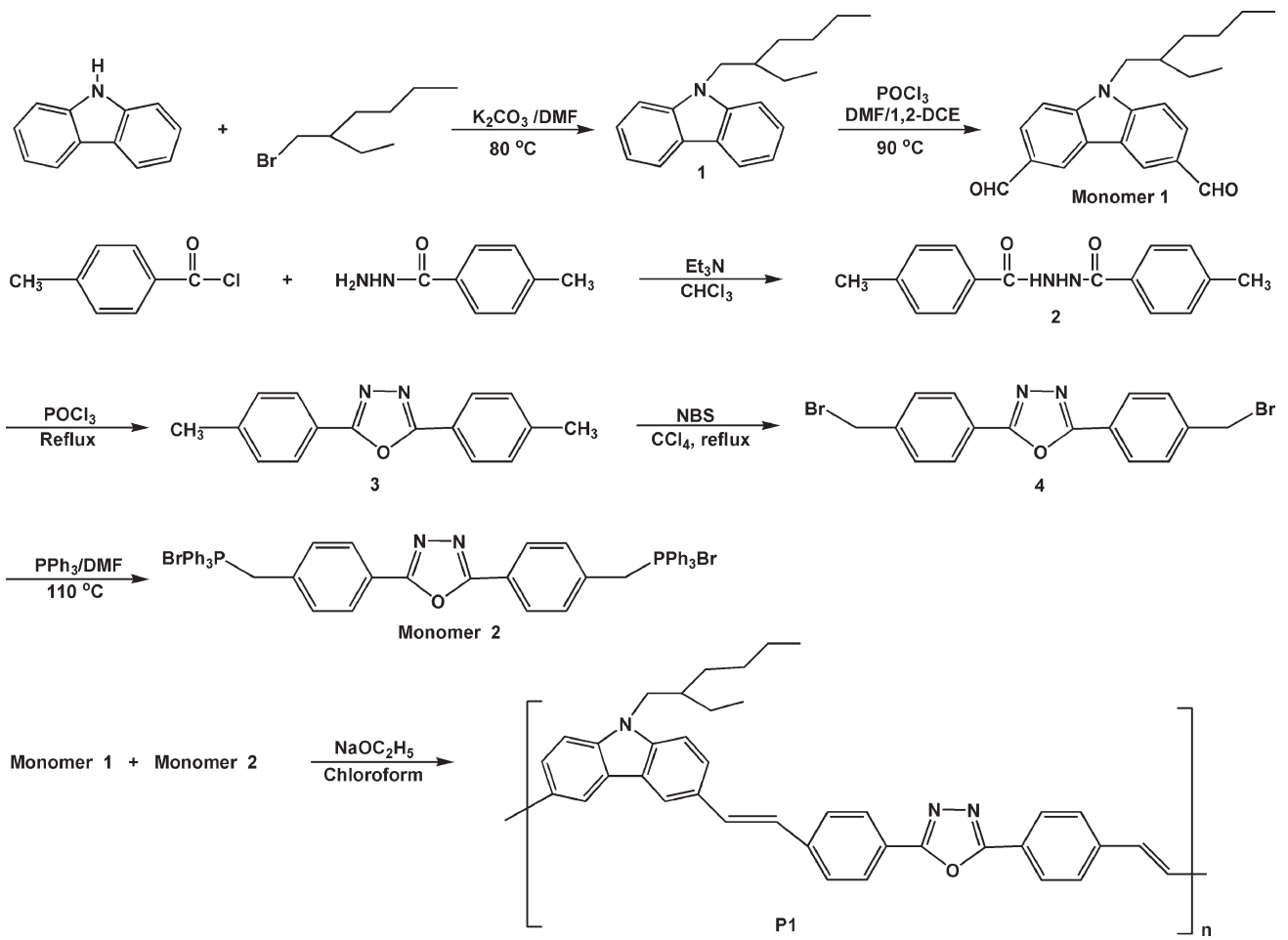

Scheme 1 Synthetic route to **P1**. 1,2-DCE: 1,2-dichloroethane, NBS: N-bromosuccinimide.

confirm polymerization. In addition, new peaks at 6.5–6.8 ppm were assigned to the formation of *cis*-vinylic linkages in all of the polymers.

Table I summarizes the polymerization results. The molecular weights and molecular weight distributions clearly showed that **P2** and **P3** obtained by the nucleophilic polycondensation had a higher molecular weight but wider molecular weight distribution than **P1** synthesized by the Witting reaction. Figure 1 shows the TGA curves of the polymers under a nitrogen atmosphere. The decomposition temperatures (T_d's), which are defined as the temperature at 5 wt % loss in TGA, were determined to be 449, 424, and 404°C for **P1, P2,** and **P3,** respectively; these values suggested good thermal stability. The differences in T_d of the polymers indicated that the full π-conjugated character of **P1** was more thermally stable than the nonconjugated flexible ether bonds of **P2** and **P3**. More importantly, the synthesized polymers exhibited high solubility in common organic solvents, such as chloroform, toluene, TCE, and THF, and showed good film quality after the spin-coating process.

Photophysical and electrochemical properties

Figures 2 and 3 show the UV–vis absorption and PL emission spectra of the polymers in both $CHCl_3$ solution and the thin-film state, respectively. Table II lists the photophysical data. **P1** showed maximum ultraviolet absorption ($\lambda_{max,UV}$) peaks at 392 nm in solution and 395 nm in the solid-film form, which might have been due to a π–π* transition along the π-conjugated backbone of carbazole and 1,3,4-oxadiazole.[29] On the other hand, **P2** and **P3** showed a blueshift in the main $\lambda_{max,UV}$ peak, with a small shoulder peak compared to **P1**. These results suggest that the insertion of an ether linkage in the π-conjugated backbone induced a blueshift in the absorption peaks, and the resulting different electronic properties also induced the appearance of a main $\lambda_{max,UV}$ peak with a shoulder peak in **P2** and **P3**.[30,31] Among them, a more blueshifted $\lambda_{max,UV}$ peak of **P2,** which was the same phenomenon reported by Xia and Advincula,[27] was attributed to the interruption of the linear π system by an N atom in the carbazole moiety.

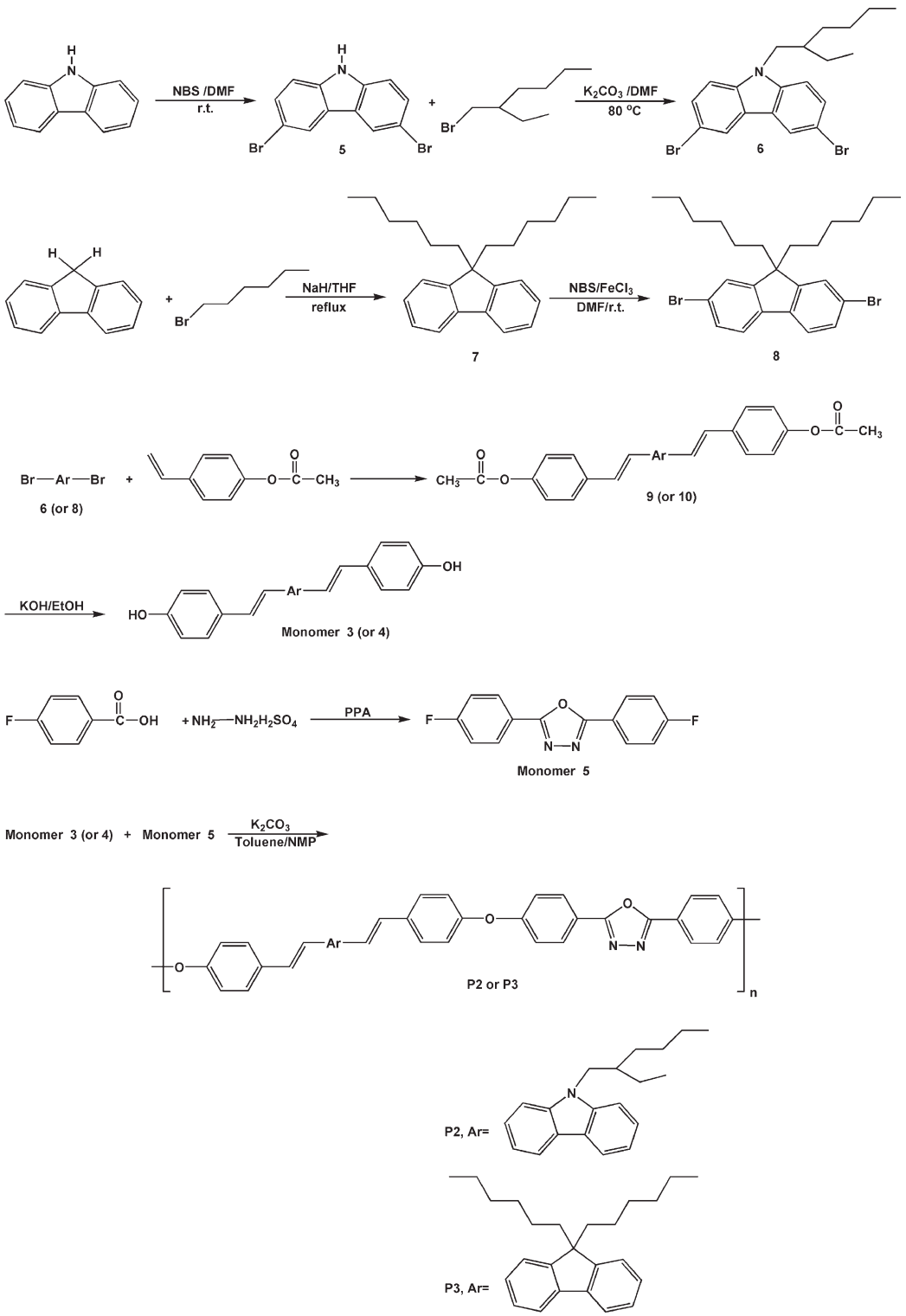

Scheme 2 Synthetic routes to **P2** and **P3**. NBS: N-bromosuccinimide; r.t.: room temperature.

The PL emission spectra of the polymers in solution or the solid state were obtained with the excitation at their $\lambda_{max,UV}$ values. The PL data in Table II show that **P1** produced green emissions with a maximum photoluminescence absorption ($\lambda_{max,PL}$) peak at 468 nm in solution and at 491 nm in the film, whereas **P2** and **P3** were both blue emitters. Their $\lambda_{max,PL}$ values in solution were measured at 407 and 414 nm for **P2** and **P3,** respectively, and at 439 and 452 nm, respectively, in their film states. Similar to those observed in the absorption spectra, the $\lambda_{max,PL}$ peaks of **P2** and **P3** were blueshifted compared to

TABLE I
Characteristics of the Polymers

Polymer	Yield (%)	M_n (g/mol)	M_w (g/mol)	M_w/M_n	T_d (°C)
P1	85	9,600	10,400	1.08	449
P2	87	28,600	43,000	1.50	424
P3	73	20,000	28,500	1.43	404

M_n = number-average molecular weight; M_w = weight-average molecular weight.

those of **P1**. The PL spectra of the polymers in the film states showed a redshift and peak broadening compared to those in solution; this could have been driven by intermolecular π–π stacking in the film states.[32]

Figure 4 shows the cyclic voltammograms of the polymers, which were obtained from the films prepared by dip-coating a Pt wire into a polymer solution. The ionization potential of the polymers [$I_{p(\text{polymer})}$] was measured to be $I_{p(\mathbf{P1})} = -5.47$ eV, $I_{p(\mathbf{P2})} = -5.59$, and $I_{p(\mathbf{P3})} = -5.81$ eV, respectively. As summarized in Table II, the I_p levels were similar to those measured with the Riken Keiki AC-2. The I_p levels of **P1** and **P2** were higher than that of **P3** because of the higher hole affinity carbazole groups in the polymer backbone. The I_p levels, especially for **P1** and **P2,** were similar to those of typical small organic hole-injection/transport N,N′-diphenyl-N,N′-(3-methylphenyl)-[1,1′-biphenyl]-4,4′-diamine (TPD) ($I_p \approx -5.5$ eV) or N′-diphenyl-N,N′-bis(1-naphthyl)(1,1′-biphenyl)-4,4′diamine (NPB) ($I_p \approx -5.7$ eV). The optical band gap energy (E_g's) of the polymers, as determined by the intersection of its absorption and emission spectra, were $E_{g(\mathbf{P1})} = 2.84$ eV, $E_{g(\mathbf{P2})} = 3.12$ eV, and $E_{g(\mathbf{P3})} = 3.05$ eV, respectively. The electron affinities (E_a's) of the polymers, as calculated from E_g, were $E_{a(\mathbf{P1})} = -2.63$ eV, $E_{a(\mathbf{P2})} = -2.47$ eV, and $E_{a(\mathbf{P3})} = -2.76$ eV, respectively. These high E_a values suggested a better exciton-blocking property than that of PEDOT–PSS ($E_a = -3.30$ eV). This point is discussed further with device performance later in the text.

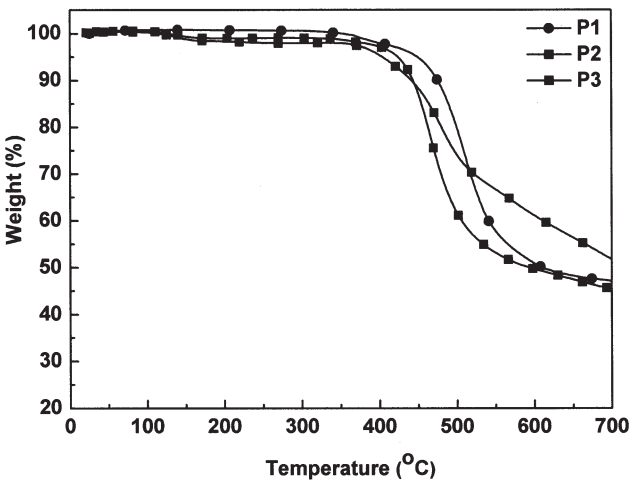

Figure 1 TGA curves of the polymers.

Performance of the devices with polymers as an HIL/HTL

The following device architectures were used. The control device (device 1) was based on ITO/PEDOT–PSS/Alq_3 (60 nm)/LiF (1 nm)/Al (100 nm), where Alq_3 acted as an emitting material, as shown in Figure 5. PEDOT–PSS was replaced with the synthesized polymer, ITO/**P1** (**P2** or **P3**)/Alq_3 (60 nm)/LiF (1 nm)/Al (100 nm), to examine the hole-injection/transport properties of the polymers in the devices. All of the devices showed bright green electroluminescence from Alq_3 at 530 nm; this indicated no significant changes in the average location of the emission zone.

Figure 6(a,b) shows the *I–V* and *L–V* properties of the devices, respectively. Table III summarizes the device performance. From the *I–V* characteristics, it was clear that *I* was high for the devices containing the synthesized polymers as the control device, and the same maximum *I* was reached, regardless of the different turn-on voltages. Because the synthesized polymer layer working as an HIL/HTL was the only variation in the device structure, the change in *I* in the *I–V* measurements was likely related to the hole-injection/transport properties of the polymer layer in the devices. These results suggest that the hole-injection/transport characteristics of the devices were not changed by the replacement of PEDOT–PSS with the synthesized polymers. Moreover, the

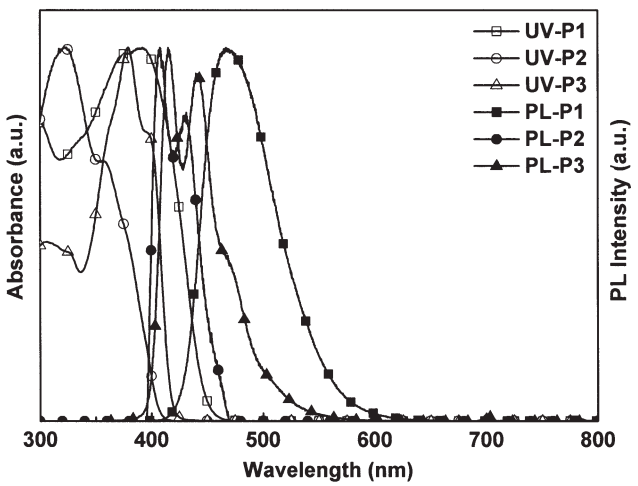

Figure 2 UV–vis absorption and PL emission spectra of the polymers in $CHCl_3$.

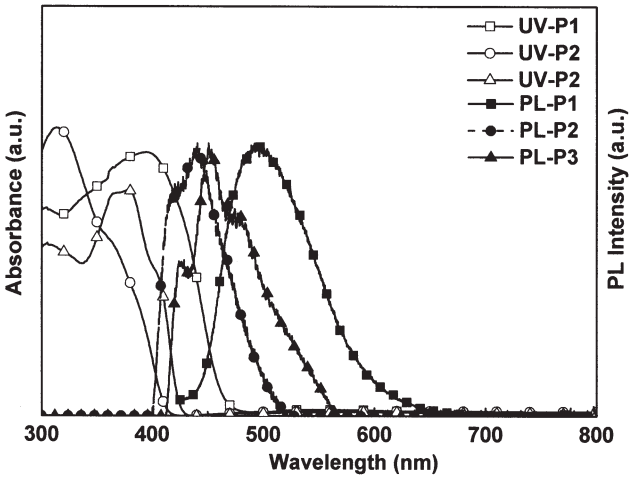

Figure 3 UV–vis absorption and PL emission spectra of the polymers in the film states.

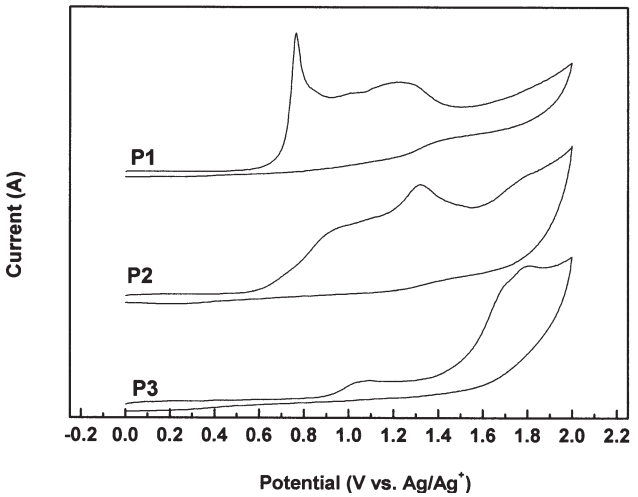

Figure 4 Cyclic voltammograms of the polymers (0.10*M* Bu_4NBF_4 in CH_3CN, scan rate = 50 mV/s).

series resistance of the devices incorporating **P1** and **P2** in the *I–V* measurements was comparable to that of the control device fabricated with PEDOT–PSS. PEDOT–PSS was reported to have ohmic contact with ITO.[33] Although the reasons for these results necessitate further study, the synthesized **P1** and **P2** were believed to make good adhesion with ITO at the interface over an identical *I*. However, the turn-on voltages of the devices fabricated with the synthesized polymers ranged from 6 to 10 V, which was higher than the 4 V measured for the control device. The order of increasing turn-on voltage was in the same order of increasing ϕ_h [$\phi_{h(\mathrm{ITO/polymer})} = \Phi_{(\mathrm{ITO})} - I_{p(\mathrm{polymer})}$, where $\Phi_{(\mathrm{ITO})}$ is the work function of ITO] from $\phi_{h(\mathrm{ITO/}\mathbf{P1})} = 0.67$ eV through $\phi_{h(\mathrm{ITO/}\mathbf{P2})} = 0.79$ eV to $\phi_{h(\mathrm{ITO/}\mathbf{P3})} = 1.01$ eV, compared to $\phi_{h(\mathrm{ITO/PEDOT–PSS})} = 0.5$ eV. Therefore, the turn-on voltage and hole injection were determined exclusively by ϕ_h at the interface between $\Phi_{(\mathrm{ITO})}$ and the I_p levels of the polymers. It was possible that the polymer/Alq_3 interface at another side, which was introduced by the replacement of PEDOT–PSS, might have affected the hole-injection characteristics. However, the ϕ_h values between the polymers and Alq_3 were lower [ranging from $\phi_{h(\mathbf{P1}/\mathrm{Alq3})} = 0.23$ eV through $\phi_{h(\mathbf{P2}/\mathrm{Alq3})} = 0.11$ eV to $\phi_{h(\mathbf{P3}/\mathrm{Alq3})} = -0.11$ eV] than that of the control device [$\phi_{h(\mathrm{PEDOT–PSS/Alq3})} = 0.4$ eV]. It appeared that the effect of ϕ_h at the polymer/Alq_3 interface on the turn-on voltage was not superficial, even when both sides of the ϕ_h values were considered. Even in the **P3**/Alq_3 interface with little ϕ_h, there was no improvement in *I* or the turn-on voltage compared to the control device. Moreover, the device prepared with **P3** exhibited a higher series resistance than the other devices. Because a higher electron-injection barrier from Alq_3 to the polymers at the polymer/Alq_3 interface was observed in the devices, on the other hand, more efficient electron/exciton blocking would have been expected at the interface between the synthesized polymers and Alq_3 layers compared to the control device. This is discussed later with the *L–V* properties of the devices.

As shown for the *L–V* properties of the devices in Figure 6(b), the *L* values of the devices prepared with the synthesized polymers were higher over the entire *I* range than those of the control device. This was another indication that the replacement of PEDOT–PSS with the synthesized polymers

TABLE II
Photophysical and Electrochemical Properties of the Polymers

	Solution		Film						
Polymer	$\lambda_{max,UV}$ (nm)	$\lambda_{max,PL}$ (nm)	$\lambda_{max,UV}$ (nm)	$\lambda_{max,PL}$ (nm)	E_{ox} (V)	I_p (eV)[a]	I_p (eV)[b]	E_g (eV)[c]	E_a (eV)[d]
P1	392	468	395	491	0.77	−5.47	−5.55	2.84	−2.63
P2	319	407	314	439	0.89	−5.59	−5.65	3.12	−2.47
P3	378	414	377	452	1.11	−5.81	−5.86	3.05	−2.76

E_{ox}, oxidation potential.
[a] Calculated from the first oxidation peak measured by cyclic voltammetry to the reference; Ag/Ag^+, $I_p = -(E_{ox} + 4.7)$ (eV).
[b] Measured with a Riken Keiki AC-2.
[c] Calculated from the intersection of the UV–vis and PL spectra.
[d] Estimated by the determination of E_g from I_p.

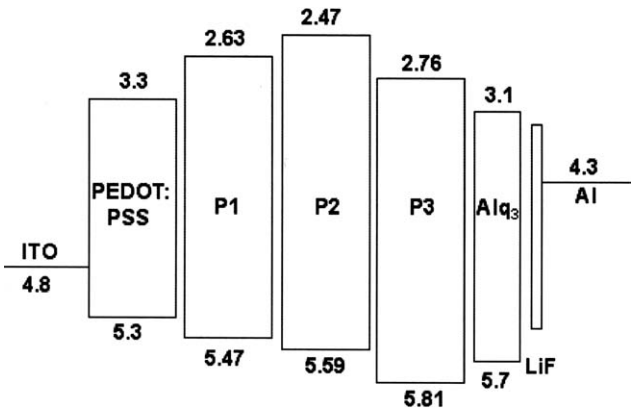

Figure 5 Schematic energy diagram of the devices (ITO/polymer/Alq_3/LiF/Al) with **P1–P3** and PEDOT–PSS as an HIL/HTL.

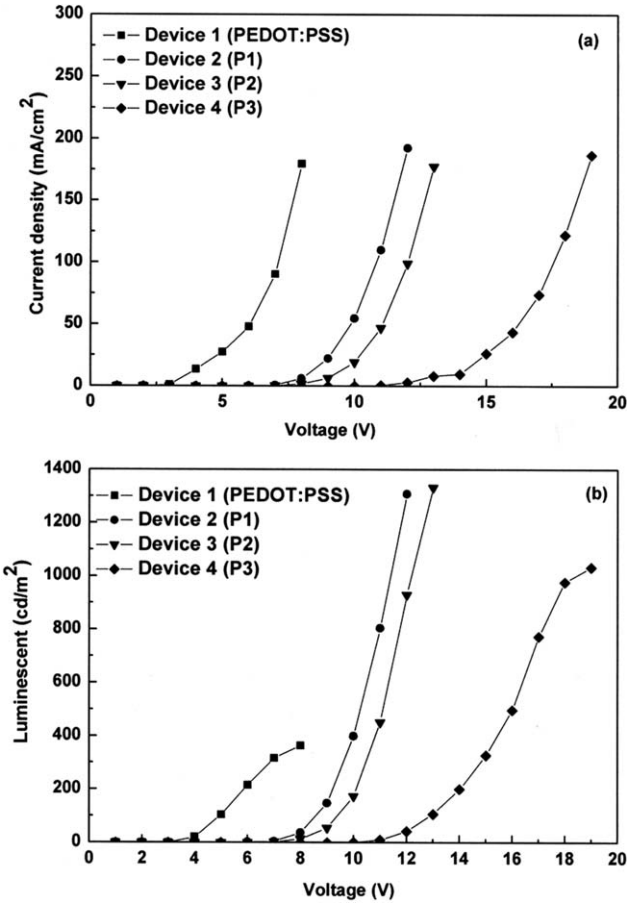

Figure 6 Performance of OLEDs fabricated with **P1–P3** as an HIL/HTL: (a) *I–V* and (b) *L–V* curves.

prevented radiative exciton quenching by the PEDOT–PSS interface[14,17–20] and improved the electron/exciton blocking by the higher E_a of the synthesized polymers compared to that of PEDOT–PSS. Further proof of the improvement in device performance by the synthesized polymers was observed in the current and power efficiencies, shown in Table III. However, not of all the device performances were satisfied because this simple double-layer device structure was not intended for practical purposes. Hence, additional improvement should be possible with further optimization of the energy levels of the devices by application of the polymers after their structural modification.

CONCLUSIONS

Conjugated copolymer (**P1**) containing *N*-(2-ethylhexyl)-3,6-carbazole–vinylene and oxadiazole groups was synthesized by the Wittig reaction. Nonconjugated copolymers (**P2** and **P3**) with flexible aryl ether units, consisting of *N*-(2-ethylhexyl)-3,6-carbazole–vinylene for **P2** and 9,9-dihexyl-2,7-fluorene–vinylene for **P3,** and an oxadiazole group were also prepared by nucleophilic polycondensation. The polymers were soluble in common organic solvents and exhibited high thermal stability in a nitrogen atmosphere. The effect of the polymers as HILs/HTLs on the device performance was examined by the fabrication of double-layer devices with the configuration ITO/polymer (**P1, P2,** or **P3**)/Alq_3/LiF/Al and comparison with that of the control device fabricated with PEDOT–PSS. The devices fabricated with the polymers showed good adhesion to the ITO anode and comparable hole-injection/transport performance compared to the control device. This also showed that the replacement of PEDOT–PSS with the synthesized polymers prevented the radiative exciton quenching caused by the PEDOT–PSS interfaces and improved the electron/exciton blocking because of the higher E_a of the synthesized

TABLE III
Electroluminescent Properties of the Devices (ITO/Polymer/Alq_3/LiF/Al) with the Polymers as HILs/HTLs

Device	Polymer	Turn-on voltage (V)	Maximum brightness (cd/m^2)	Current efficiency (cd/A)	Power efficiency (lm/W)
Device 1	PEDOT:PSS	4	364	0.20	0.07
Device 2	**P1**	6	1309	0.68	0.11
Device 3	**P2**	7	1333	0.75	0.28
Device 4	**P3**	10	1034	0.55	0.10

polymers; this resulted in higher electroluminescence under an identical device structure.

References

1. Shen, Z.; Burrows, P. E.; Bulovic, V.; Forrest, S. R.; Thompson, M. E. Science 1997, 276, 2009.
2. Bernius, M. T.; Inbasekaran, M.; O'Brien, J.; Wu, W. Adv Mater 2000, 12, 1737.
3. Pei, Q.; Yang, Y. J Am Chem Soc 1996, 118, 7416.
4. Ranger, M.; Rondeau, D.; Leclerc, M. Macromolecules 1997, 30, 7686.
5. Rehahn, M.; Schlüter, A. D.; Wegner, G.; Feast, W. J. Polymer 1989, 30, 1054.
6. Su, W.-F.; Yeh, K.-M.; Chen, Y. J Polym Sci Part A: Polym Chem 2007, 45, 4377.
7. Suzuki, A.; Miyaura, N. Chem Rev 1995, 95, 2457.
8. Jung, S. H.; Kim, H. K.; Kim, S. H.; Jeong, S. C.; Kim, Y. H.; Kim, D. Macromolecules 2000, 33, 9277.
9. Yang, Z.; Hu, B.; Karasz, F. E. Macromolecules 1995, 28, 6151.
10. Ishii, H.; Sugiyama, K.; Ito, E.; Seki, K. Adv Mater 1999, 11, 605.
11. Braun, S.; Salaneck, W. R.; Fahlman, M. Adv Mater 2009, 21, 1450.
12. Ho, P. K. H.; Kim, J.-S.; Burroughes, J. H.; Becker, H.; Li, S. F. Y.; Brown, T. M.; Cacialli, F.; Friend, R. H. Nature 2000, 404, 481.
13. Xu, Q.; Ouyang, J.; Yang, Y.; Ito, T.; Kido, J. Appl Phys Lett 2003, 83, 4695.
14. Kim, J.-S.; Ho, P. K. H.; Murphy, C. E.; Seeley, A. J. A. B.; Grizzi, I.; Burroughes, J. H.; Friend, R. H. Chem Phys Lett 2004, 386, 2.
15. Poplavskyy, D.; Nelson, J.; Bradley, D. D. C. Appl Phys Lett 2003, 83, 707.
16. Poplavskyy, D.; Su, W.; So, F. J Appl Phys 2005, 98, 014501.
17. Vitoratos, E.; Sakkopoulos, S.; Dalas, E.; Paliatsas, N.; Karageorgopoulos, D.; Petraki, F.; Kennou, S.; Choulis, S. A. Org Electron 2009, 10, 8.
18. Okachi, T.; Nagase, T.; Kobayashi, T.; Naito, H. Thin Solid Films 2008, 517, 1327.
19. Kim, J.-S.; Friend, R. H.; Grizzi, Z.; Burroughes, J. H. Appl Phys Lett 2005, 87, 023506.
20. Chen, A. C. A.; Wallace, J. U.; Klubek, K. P.; Madaras, M. B.; Tang, C. W.; Chen, S. H. Chem Mater 2007, 19, 4043.
21. Choulis, S. A.; Choong, V.-E.; Mathai, M. K.; So, F. Appl Phys Lett 2005, 87, 113503.
22. Harding, M. J.; Poplavskyy, D.; Choong, V.-E.; So, F.; Campbell, A. J. Proc SPIE 2006, 6333, 63331M.
23. Jin, Y.; Kim, J. Y.; Park, S. H.; Kim, J.; Lee, S.; Lee, K.; Suh, H. Polymer 2005, 46, 12158.
24. van Dijken, A.; Bastiaansen, J. J. A. M.; Kiggen, N. M. M.; Langeveld, B. M. W.; Rothe, C.; Monkman, A.; Bach, I.; Stössel, P.; Brunner, K. J Am Chem Soc 2004, 126, 7718.
25. Shia, J.; Huang, M. M.; Xina, Y. R.; Chen, Z. J.; Gong, Q.; Xu, S.; Cao, S. K. Mater Lett 2005, 59, 2199.
26. Peng, Z.; Bao, Z.; Galvin, M. E. Adv Mater 1998, 10, 680.
27. Xia, C.; Advincula, R. C. Macromolecules 2001, 34, 5854.
28. Lee, J. K.; Klaerner, G.; Miller, R. D. Chem Mater 1997, 11, 1083.
29. Jin, Y.; Kim, J. Y.; Park, S. H.; Kim, J.; Lee, S.; Lee, K.; Suh, H. Polymer 2005, 46, 12158.
30. Chowchows, C. L.; Ovaries, G. K.; Kokkali, F.; Yiannoulis, P.; Kallitsis, J. K.; Gregoriou, P V. G. Polymer 2005, 46, 4654.
31. Peeters, E.; van Hal, P. A.; Knol, J.; Brabec, C. J.; Sariciftci, N. S.; Hummelen, J. C. J Phys Chem B 2000, 104, 10174.
32. Chen, Y.; Hwang, S.-W.; Yu, Y.-H. Polymer 2003, 44, 3827.
33. Campbell, A. J.; Bradley, D. D. C.; Antoniadis, H.; Inbasekaran, M.; Wu, W. W.; Woo, E. P. Appl Phys Lett 2000, 76, 1734.